PNAS RESEARCH ARTICLE | ECOLOGY

Forest biodiversity increases productivity via complementarity from greater canopy structural complexity

Xianglu Deng[a,b], Bernhard Schmid[c], Helge Bruelheide[d,e], Chen Chen[a], Yi Li[a], Shan Li[a], Felix Morsdorf[c], Tama Ray[d,e,f], Meredith C. Schuman[c,g], Ting Tang[a,c], Goddert von Oheimb[f], Keping Ma[a], and Xiaojuan Liu[a,b,h,1]

Affiliations are included on p. 9.

Edited by David Tilman, University of Minnesota College of Biological Sciences, St. Paul, MN; received April 1, 2025; accepted August 28, 2025

The horizontal distribution and vertical stratification of tree crowns can affect light interception and tree growth, thus driving forest productivity and carbon storage. However, how canopy structure is affected by tree diversity and thus can mediate its effects on productivity remains unclear. Using 4-y consecutive unmanned aerial vehicle-borne light detection and ranging and ground-based growth measurements from 482 plots and 38,088 trees, 11 to 15 y after planting, within a large-scale forest biodiversity experiment in southeast China, we found that increased canopy structural complexity consistently explains the positive effects of tree diversity on productivity. Species complementarity was the main mediator of diversity-enhanced productivity, with the positive complementarity effects strengthening over time. Our study underscores the importance of establishing multispecies forest communities with complex canopy structure to maximize productivity and carbon sequestration in forest ecosystems.

biodiversity–ecosystem functioning (BEF) | complementarity effects | canopy structural complexity | forest aboveground biomass | UAV-borne LiDAR

Significance

A more complex canopy structure enhances both light use and productivity in forests. Applying unmanned aerial vehicle-borne laser scanning across a large forest biodiversity experiment in southeast China (BEF-China), we found that tree diversity consistently promoted aboveground biomass through fostering complex canopy structures. With advancing forest age, the positive relationship between canopy structural complexity and forest biomass was increasingly associated with enhanced species complementarity. Our work underscores the importance of longer experimental durations to reveal mechanisms underpinning forest diversity–productivity relationships.

Numerous studies have documented positive biodiversity–productivity relationships in both observational and experimental forest biodiversity studies (1, 2). In forest ecosystems, the arrangement and occupancy of canopy components in three-dimensional (3D) space, defined as canopy structural complexity (CSC) (3), may be a key mediator of these positive biodiversity–productivity relationships. This is because greater CSC—including both horizontal distribution and vertical stratification (3, 4)—can improve light interception and absorption (5), which in turn increases resource-use efficiency and community productivity (6, 7). Species-rich forests tend to be more structurally complex due to interspecific differences in tree functional traits and diversity-induced shifts in crown morphology and biomass allocation patterns (8, 9), which promote the physical occupancy and niche partitioning in canopy space (hereafter, crown complementarity). Studies based on observational data in natural forests are generally unable to rigorously test the causality of these relationships because of the effect of confounding variables. Experimental investigations on how tree diversity affects CSC across horizontal and vertical dimensions as well as 3D space are critical for understanding its potential role as a mediator of biodiversity–productivity relationships. However, previous biodiversity studies (7, 10, 11) were limited to short-term experiments, spanning only a few growing seasons or a narrow gradient of tree species richness, which may primarily reflect initial processes such as selection effects (SE) (12, 13). Longer-term biodiversity experiments are needed as diversity effects and their underlying mechanisms change over time (14). Slow tree growth implies that years or decades may be needed to observe effects of niche partitioning (15). Therefore, processes such as species complementarity [captured by complementarity effects (CE)] (13) in the filling of canopy space may take more time to develop (16, 17) and only become detectable given sufficiently long experimental durations.

Horizontal and vertical structural elements refer to different facets of forest structure, with horizontal structure including size differentiation, distribution patterns, and crowding, and vertical structure including stratification of forest layers (18). Quantifying horizontal and vertical structure thus provides information of complementary canopy structure, and is essential for understanding the role of CSC in regulating species interactions and stand productivity (19, 20). CSC has traditionally been quantified by several one- or two-dimensional parameters, including canopy height and openness (21, 22), derived from field inventories. Advances in light detection and ranging (LiDAR) technology have made it possible to accurately capture multidimensional attributes of CSC (3, 23). More recently, unmanned aerial vehicles (UAV) with LiDAR sensors provide high spatial resolution point cloud that enable precise estimation of canopy structural attributes, allowing

Author contributions: X.L. designed research; X.D. and X.L. performed research; X.D., T.T., and X.L. analyzed data; and X.D., B.S., H.B., C.C., Y.L., S.L., F.M., T.R., M.C.S., T.T., G.v.O., K.M., and X.L. wrote the paper.

The authors declare no competing interest.

This article is a PNAS Direct Submission.

[1]To whom correspondence may be addressed. Email: liuxiaojuan06@ibcas.ac.cn.

This article contains supporting information online at https://www.pnas.org/lookup/suppl/doi:10.1073/pnas.2506750122/-/DCSupplemental.

Published October 1, 2025.

better characterization of both horizontal and vertical canopy structure (24, 25). For example, canopy cover derived from UAV-borne LiDAR measurements and indicative of canopy openness, can be used as an indicator of horizontal canopy structure; foliage height diversity (FHD), which represents the number and variation of canopy layers, can indicate vertical CSC. In addition, a holistic approach based on fractal analysis, the box dimension (D_b), was applied to characterize the 3D structural complexity of the canopy (26, 27). The box dimension is a multiscale metric that constructs a sequence of 3D grids dividing canopy space into homogeneous voxels of decreasing size, counting the number of occupied voxels at each scale. This approach integrates the distribution and density of canopy structural elements in 3D space across spatial scales (28). The UAV-borne LiDAR data, in conjunction with appropriate field surveys, can provide a detailed, multifaceted interpretation of forest structure, offering a powerful approach for experimental biodiversity–ecosystem functioning research (29, 30).

The relationship between tree species richness and CSC is generally positive across scales, including the neighborhood (8) and community scales (31, 32). Species-specific differences in crown architecture, growth rates, and leaf physiology not only result in horizontal heterogeneity but also in vertical stratification (33, 34). In addition, neighborhood interactions in mixed-species communities alter tree crowns and biomass allocation via morphological plasticity (8, 9, 35). Both facets of crown complementarity, species-specific differences and morphological plasticity, can improve the efficient use of canopy space. Moreover, positive effects of tree species richness on CSC have been observed to increase over time (36). A more complex canopy, and thus higher canopy packing (36), can lessen the competition for light and improve light interception efficiency, and is therefore likely to promote important ecosystem functions, particularly productivity (5). Nevertheless, some studies from natural forests have observed nonsignificant or even negative relationships between CSC and community productivity (37, 38). Asymmetric light competition between overstory and understory layers may reduce light availability and suppress growth in the understory, thereby lowering overall community productivity in structurally complex forests (37, 39). These divergent effects of CSC on productivity may be due to the covariation of CSC and productivity with various environmental gradients in observational studies (40). Here, we try to clarify how CSC modulates the biodiversity–productivity relationships in a large biodiversity experiment using techniques that allow detailed characterization of canopy occupancy in multidimensional space.

We used consecutive UAV-borne LiDAR and field inventory data collected from 2021 to 2024 in a forest biodiversity experiment planted in 2009 in subtropical China (BEF-China) (2, 41). The dataset included 482 plots of 1 mu (25.8 m × 25.8 m, i.e., 0.067 ha), each planted with 400 trees in monocultures and 2-, 4-, 8-, 16-, and 24- species mixtures (Fig. 1*A*). We calculated cumulative aboveground biomass for each plot based on field measurements of stem diameter and height to indicate tree growth. In addition, we followed Loreau and Hector (13) to mathematically partition the net biodiversity effects of community productivity into CEs and SEs for each mixture in each year. Positive CEs occur when most species in a mixture contribute more than expected based on their monoculture values to a community-level function such as productivity. Positive SEs are caused by a few species with high values in monoculture, which also contribute to the high values in mixtures (13, 15). Note that SEs are zero if all monocultures have the same value, e.g. for productivity. While CEs and SEs cannot directly be equated with ecological mechanisms, such as an increase in CSC, we would expect them to be correlated to some degree with CSC, reflecting potential pathways. Three indices of CSC were derived from UAV-borne LiDAR data, including canopy cover to represent the horizontal distribution, FHD to describe the vertical complexity, and box dimension to summarize the holistic 3D CSC. We tested the following hypotheses (Fig. 1*B*). H1: Tree species richness increases CSC, based on evidence that tree species differ in crown architecture and growth strategies (31, 32). H2: CSC increases community aboveground biomass (H2-1) due to greater resource-use efficiency (7, 11) and mediates the effects of tree species richness on community aboveground biomass (H2-2). H3: Higher CSC and higher productivity in more diverse experimental plots are related more to CEs than SEs (35). For all three

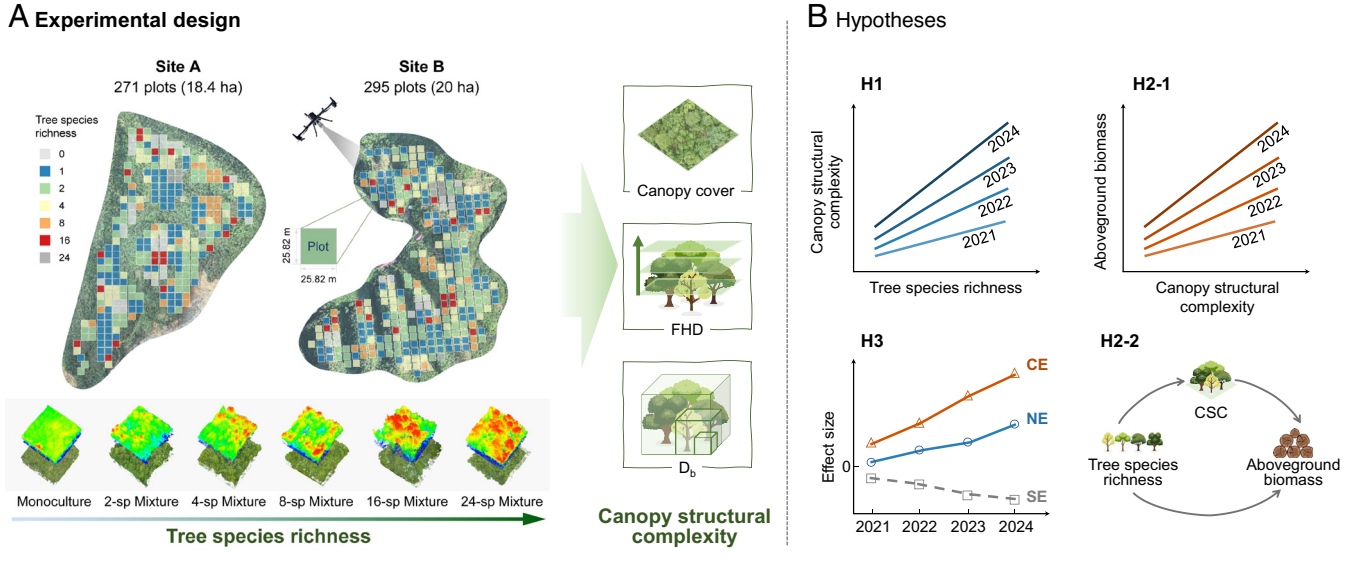

Fig. 1. Experimental design and hypotheses of this study. (*A*) Study sites and measurements. Diversity design of BEF-China and the CSC measurements, including canopy cover, FHD, and box dimension (D_b). (*B*) Hypotheses: H1, tree species richness increases CSC; H2, CSC increases community aboveground biomass (H2-1). In particular, CSC is a mediator of the effects of tree species richness on community aboveground biomass (H2-2); and H3, higher CSC and higher productivity in more diverse experimental plots are related more to CE than SE—two additive components of net biodiversity effect (NE). For all three hypotheses we use the multiple years of measurements to assess the consistency of results; and, in addition, we predict that the effects increase over time.

hypotheses we use the multiple years of measurements to assess the consistency of results; and, in addition, we predict that the effects increase over time.

Results

Relationships Between Tree Species Richness, CSC, and Community Aboveground Biomass. Overall, tree species richness had significant positive effects on all three CSC indices (all $P < 0.001$; Fig. 2 and *SI Appendix*, Table S1). The positive effects of tree species richness on canopy cover decreased over time while remaining consistent on FHD and box dimension ($P < 0.001$; Fig. 2 and *SI Appendix*, Table S1). In the last year of the study period, 2024, canopy cover, FHD, and box dimension were on average 13%, 21%, and 10% higher, respectively, in 24-species mixtures than in the average monocultures (all $P < 0.001$; Fig. 2). Community aboveground biomass, calculated from the accumulated aboveground volume of trees at the plot level based on field measurements (not LiDAR data), significantly increased with all CSC indices (all $P < 0.001$; Fig. 3 and *SI Appendix*, Table S2). In 2024, aboveground biomass was over three times higher (+335%) in communities with high FHD (95% quantile of FHD = 2.7) than in communities with low FHD (5% quantile of FHD = 1.7). Furthermore, the positive relationships between CSC indices and aboveground biomass strengthened over time, as indicated by significant two-way interactions of year as continuous variable and CSC indices (all $P < 0.001$; *SI Appendix*, Table S2).

Contribution of CSC to Species Richness Effects on Community Aboveground Biomass. To examine the contribution of CSC to the tree species richness effects on community aboveground biomass, we compared the relationships between tree species richness and aboveground biomass with and without accounting for potential mediation through CSC as covariate. When the 3D CSC index, i.e., box dimension, was absent from models, tree species richness had significant positive effects on aboveground biomass in every year from 2021–2024 (all $P < 0.001$; Fig. 4*A* and *SI Appendix*, Tables S3 and S4). However, when box dimension was included as covariate in the models, the positive effects of tree species richness became nonsignificant (all $P > 0.1$; Fig. 4*A* and *SI Appendix*, Tables S3 and S4), and the residual direct effect in 2021 became even significantly negative ($P < 0.05$; Fig. 4*A* and *SI Appendix*, Table S4), suggesting that the richness effects on aboveground biomass were mediated by the covariate.

We next fitted structural equation models (SEMs) to disentangle the multivariate relationships among tree species richness, box dimension, and aboveground biomass. The final SEM of the latest year fitted the data well (Fisher's C = 0.87, DF = 2, $P = 0.65$) and explained 57% of the variation in aboveground biomass (Fig. 4*B* and *SI Appendix*, Table S5). The SEM revealed that aboveground biomass directly increased with box dimension, i.e., the holistic 3D structural complexity, with the coefficient of r = 0.75 ($P < 0.001$; Fig. 4*B* and *SI Appendix*, Table S5). Additionally, box dimension increased with tree species richness (r = 0.39, $P < 0.001$), which led to positive indirect effects of tree species richness on aboveground biomass (Fig. 4*B* and *SI Appendix*, Table S5). Similarly, the final SEMs for the years 2021, 2022, and 2023 also showed good fits to the data, with similar paths as the one of 2024 (*SI Appendix*, Fig. S2 and Table S5).

Furthermore, we examined the role of canopy cover and FHD, i.e., the horizontal and vertical CSC indices, in mediating the positive biodiversity–productivity relationships. Including canopy cover and FHD as covariates in the models, the previously positive effects of tree species richness on aboveground biomass again turned to nonsignificant for the first two years of measurements. However, in the third and fourth year, the remaining effects of species richness on aboveground biomass in the models with the covariates was less reduced and remained significantly positive ($P < 0.01$; *SI Appendix*, Fig. S1 and Tables S3 and S4).

We again fitted SEMs to disentangle the multiple relationships among tree species richness, canopy cover, FHD, and aboveground biomass. The final SEM of the last year fitted the data well and explained 37% of the variation in aboveground biomass (Fig. 4*B* and *SI Appendix*, Fig. S3 and Table S6). The SEM revealed that aboveground biomass directly increased with canopy cover and FHD, with coefficients of r = 0.45 ($P < 0.001$), and r = 0.14 ($P = 0.003$), respectively (Fig. 4*B* and *SI Appendix*, Table S6). Additionally, canopy cover and FHD increased with tree species richness (r = 0.24, $P < 0.001$; r = 0.31, $P < 0.001$), leading to positive indirect effects of tree species richness on aboveground

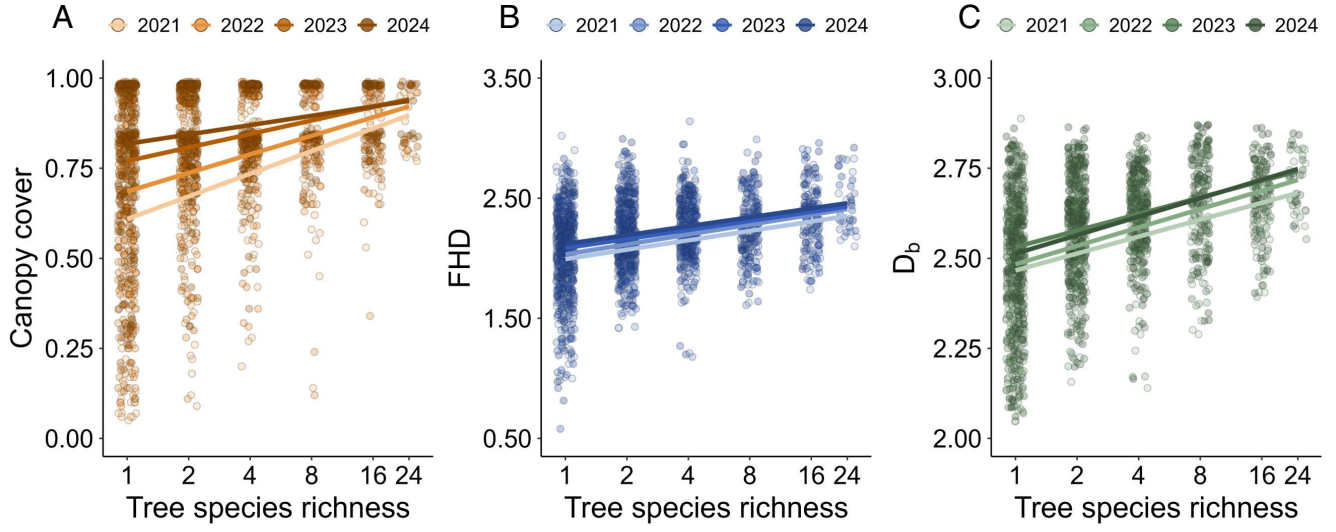

Fig. 2. Relationships between tree species richness and CSC indices from 2021–2024 (*A*–*C*). Each point represents a plot. Data points and regression lines are colored according to years, with lighter colors indicating earlier years. All relationships were significant in linear mixed models at $P < 0.001$. The *x*-axis for tree species richness was $\log_2$-transformed to linearize relationships. Analyses of variance tables for the fitted models are presented in *SI Appendix*, Table S1. FHD: foliage height diversity; D_b: box dimension.

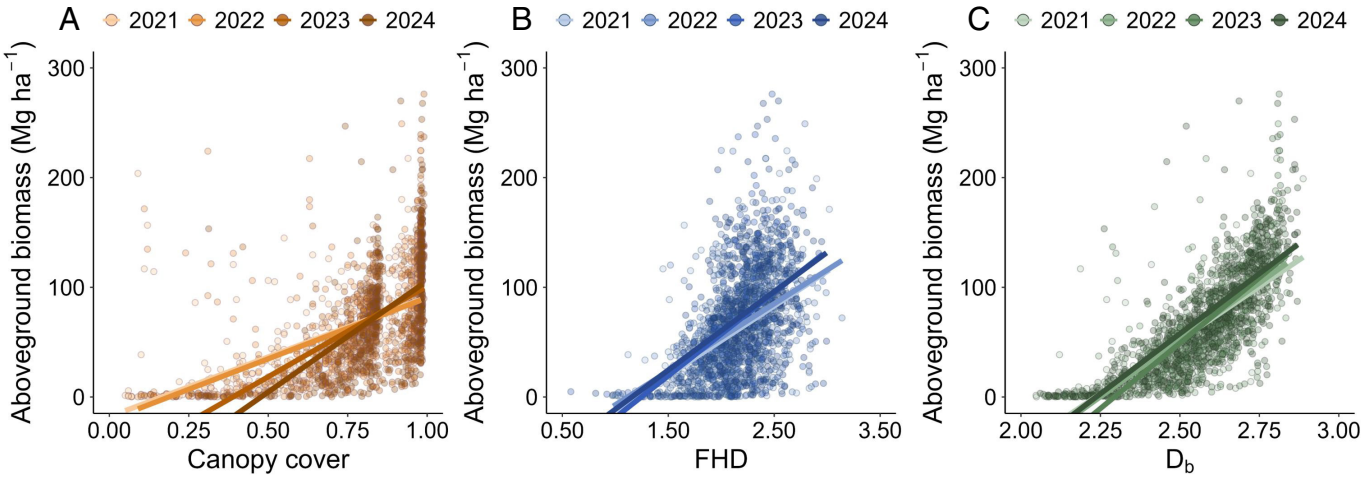

Fig. 3. Relationships between CSC indices and community aboveground biomass from 2021–2024 (*A*–*C*). Each point represents a plot. Data points and regression lines are colored according to years, with lighter colors indicating earlier years. All relationships were significant in linear mixed models at $P < 0.001$. Analyses of variance tables for the fitted models are presented in *SI Appendix*, Table S2. FHD: foliage height diversity; D_b: box dimension.

biomass (Fig. 4*B* and *SI Appendix*, Table S6). Furthermore, tree species richness had a positive direct effect on aboveground biomass (r = 0.15, $P < 0.001$; Fig. 4*B* and *SI Appendix*, Table S6).

Relationships Between CSC and CEs and SEs. Further, we assessed the relationships between CSC and net biodiversity effects (of tree species richness on community aboveground biomass) and their additive components, CEs and SEs. Net biodiversity effects were significantly positively related with all three CSC indices, i.e., canopy cover, FHD, and box dimension, in every year from 2021 to 2024 (all $P < 0.05$; Fig. 5 and *SI Appendix*, Tables S7 and S8), which was mainly due to the significant positive relationships between CSC indices and CEs (all $P < 0.05$; Fig. 5 and *SI Appendix*, Tables S7 and S8). In contrast, the relationships between CSC indices and SEs were weak ($P > 0.05$); and if marginally significant ($P < 0.1$) they were negative (Fig. 5 and *SI Appendix*, Tables S7 and S8). Moreover, we tested the relationships between tree species richness and net biodiversity effects, CEs and SEs. Net biodiversity effects and CEs increased with tree species richness from 2021 to 2024 ($P < 0.001$; *SI Appendix*, Fig. S5 and Table S11), while SEs were never significant ($P > 0.05$; *SI Appendix*, Fig. S5 and Table S11). This suggests that the overyielding of mixtures,

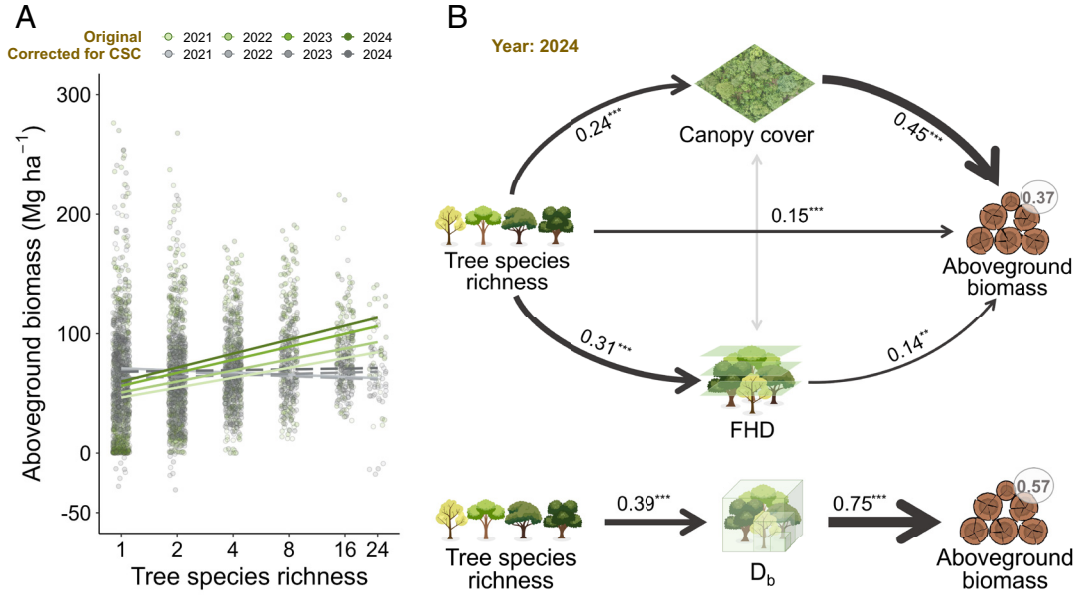

Fig. 4. Effects of CSC on tree species richness–community aboveground biomass relationships from 2021 to 2024. (*A*) Effects of tree species richness on community aboveground biomass without (green points and lines) or with CSC used as covariate (gray points and lines). Each point represents a plot. Linear mixed models were used to assess statistical significance, with solid lines representing significant relationships (all $P < 0.001$) and dashed lines indicating nonsignificant ones (all $P > 0.10$). The *x*-axis for tree species richness was $\log_2$-transformed to linearize relationships. Data points and regression lines are colored according to years, with lighter colors indicating earlier years. Gray points were obtained by the sum of overall mean community aboveground biomass and residuals from models of community aboveground biomass regressed on CSC. The extremes of the point cloud taper off toward higher diversity levels because of decreasing sample size; quantile regressions show qualitatively the same positive relationships for the largest 10% of values at each diversity level (*SI Appendix*, Fig. S4). (*B*) *Top*: structural equation model relating tree species richness via horizontal and vertical CSC indices with community aboveground biomass for 2024 (FHD). *Bottom*: structural equation model relating tree species richness via the holistic 3D CSC index (D_b: box dimension) with community aboveground biomass for 2024. The black arrows indicate positive relationships (* $P < 0.05$, ** $P < 0.01$, and *** $P < 0.001$). Arrow widths are proportional to standardized path coefficients. The conditional R^2 values are displayed next to community aboveground biomass. Details of the fitted models are given in *SI Appendix*, Tables S3–S6.

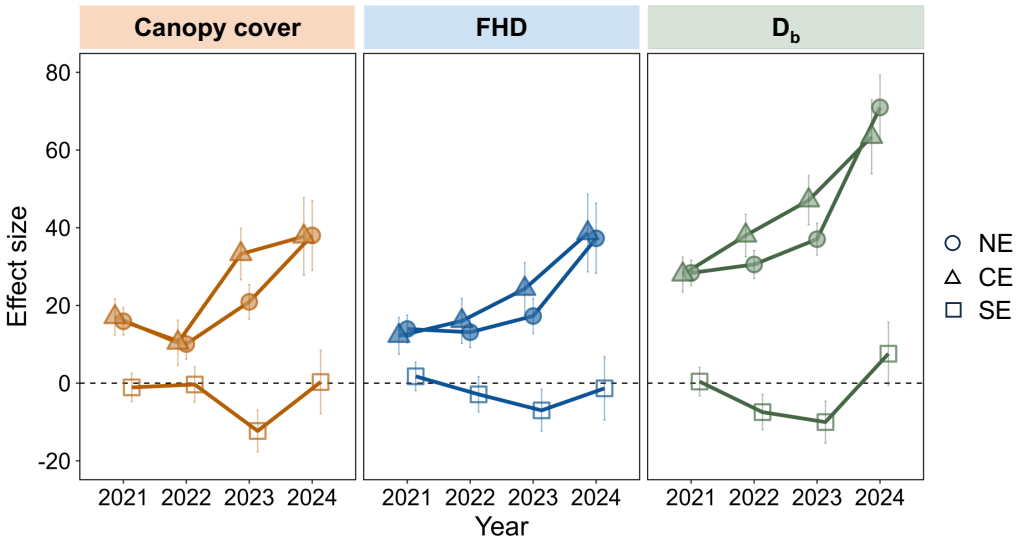

Fig. 5. Relationships between CSC indices and biodiversity effects from 2021 to 2024. Effect sizes are the coefficients of linear relationships between net biodiversity effect (NE), CE, and SE and CSC indices, i.e., canopy cover, FHD, and box dimension (D_b). Filled symbols indicate significant differences from zero ($P < 0.05$) and unfilled symbols indicate nonsignificant differences from zero ($P > 0.05$). Details of the models are provided in *SI Appendix*, Tables S7 and S8.

mediated by high CSC index values, was underpinned by species complementarity related to niche partitioning in canopy space. Such niche partitioning between tree species could be due to both preexisting genetic differences between species and differences between species that were enhanced by morphological plasticity (35), yet we lack the data to separate the two. Additionally, the positive relationships between the three CSC indices and CEs strengthened from year to year (all $P < 0.001$; *SI Appendix*, Table S7), suggesting that species complementarity, i.e. presumed niche partitioning in canopy space, continued to increase during stand development.

Discussion

In this study of a large subtropical forest biodiversity experiment, we tested the potential role of CSC in mediating tree biodiversity–productivity relationships. We found that, from 2021 to 2024 (age 11/12–14/15 of the experiment), tree species richness consistently increased CSC (H1), which in turn was positively related to community aboveground biomass (H2-1). Tree species richness increased aboveground biomass via multifaceted canopy structures across the 4 y (H2-2). The overyielding observed in species mixtures was primarily driven by stronger CEs but not SEs in structurally more complex tree communities over the 4 y (H3). Overall, our results demonstrate that CSC correlates strongly with increases of community aboveground biomass in species-diverse tree communities, suggesting that CSC may be an important mechanism underlying positive biodiversity–productivity relationships in forests.

Tree Species Richness Increases CSC. As predicted, we found significant positive effects of tree species richness on multidimensional CSC indices (i.e., canopy cover, FHD, and box dimension)—encompassing horizontal, vertical, and holistic 3D canopy structures—across a broad diversity gradient over the 4 y, indicating that mixed-species forests tend to use canopy space more efficiently than monocultures (33, 34). These positive effects may arise from genetically determined differences in crown shape between species (31, 42) and/or morphological plasticity increasing niche partitioning between species in canopy space in more species-rich communities (8, 35, 43), with components reflecting horizontal and vertical canopy packing (43, 44). This aligns with previous studies illustrating positive relationships between tree species richness and components of CSC, such as mean canopy height, canopy cover, and a stand structural complexity index, in both natural and experimental forests (7, 33, 45). However, observational studies have often neglected the vertical variation within multiple canopy layers, which is difficult to measure with traditional field inventories, especially in dense forests. Furthermore, without isolating one from the environmental context and the covariates that influence both, and demonstrating that they vary independently of each other, e.g. by preceding it in time (46), observational studies cannot decipher the direction of causality in the relationships between tree species richness and CSC. Our experimental study provides empirical evidence that greater tree species richness increases multifaceted CSC, thus confirming our first hypothesis H1, along a broad diversity gradient for more than 400 experimental plots comprising 38,088 trees over 4 y, enabled by high spatial resolution UAV-borne LiDAR.

CSC Increases Community Aboveground Biomass. Our results showed positive relationships between horizontal, vertical, and 3D CSC with community aboveground biomass calculated based on field measurements across all 4 y, consistent with other studies showing positive relationships between CSC and tree productivity (20, 47). Extending previous findings (5, 10), our results indicate that positive diversity effects on community biomass can be mediated by both denser horizontal crown packing and vertical stratification within the canopy, which can subsequently enable more effective light acquisition in mixed-species forests. The complementary use of canopy space and spatial light partitioning likely underlies the significant relationships between CSC and overyielding (20, 47). Morphological diversification between species in canopy structure can lower interspecific competition for light (48, 49) and increase overall light interception and light-use efficiency, which are essential for promoting tree growth in forests. Therefore, our results suggest that forest managers should consider increasing CSC by selective harvesting and replanting diverse species to maintain high productivity over longer time spans.

Temporal Trends in Effects of Tree Species Richness on CSC. Although our observations covered a relatively short time period during 12 to 15 (site A) or 11 to 14 (site B) years after planting, the effects of tree species richness on CSC and the relationships between CSC and community aboveground biomass showed clear linear temporal trends (*SI Appendix*, Tables S1 and S2). While the effect of tree species richness on FHD and box dimension remained relatively stable, its influence on canopy cover weakened over the years. Once the canopy closes and stratification is fully established, species richness effects on CSC may no longer increase as available space and resources become fully utilized. Furthermore, the diminishing effect of tree species richness on canopy cover suggests that the horizontal expansion of the canopy takes longer in less than in more diverse mixtures. That is, as canopy cover approaches saturation over time, stands with initially higher canopy cover are gradually "caught up" by those with lower canopy cover. The associations of canopy cover, FHD, and box dimension with community aboveground biomass strengthened over time, possibly due to the cumulative nature of our measure of community productivity, i.e. the increasing aboveground biomass over the years. These results offer evidence of temporal changes in the relationships between tree species richness, components of CSC, and community aboveground biomass in a forest biodiversity experiment. As other forest biodiversity experiments will reach similar ages, it will be interesting to see whether our present findings can be extrapolated to other environmental contexts, e.g. temperate forests with generally lower tree species richness.

Tree Species Richness Increases Community Aboveground Biomass via CSC. Structural equation models indicated that the positive effect of tree species richness on community aboveground biomass was mediated by multifaceted CSC in all years studied, from 2021 to 2024, confirming our second hypothesis H2. When the effect of tree species richness on holistic 3D CSC, i.e., box dimension, was accounted for by using it as a covariate, the remaining effect of tree species richness on aboveground biomass was no longer positive. This suggests that CSC is an important mediator underlying biodiversity–productivity relationships in more than a decade old experimental tree communities, extending findings from earlier stages of a temperate forest biodiversity experiment (7). Additionally, we found that aboveground biomass was related to diversity-driven shifts in both horizontal and vertical dimensions, i.e., canopy cover and FHD. However, after including covariates reflecting horizontal and vertical CSC components as mediators, the remaining effects of tree species richness on aboveground biomass remained positive at least in the third and fourth year of measurements. This suggests the existence of other potential pathways through which tree diversity may increase productivity in the longer term, for example, additional components of 3D CSC, belowground resource partitioning (50), increased bacterial or arthropod diversity (51, 52), or changed microclimate (53).

Compared with previous studies in temperate and tropical ecosystems (7, 47), our findings additionally show that the horizontal distribution and vertical stratification of forest canopies together can explain the positive effects of tree diversity on productivity in subtropical forests along a broad diversity gradient. The increase in canopy cover with tree species richness suggests that it allows trees to occupy additional space through lateral crown expansion in mixtures (34). This corresponds with the idea that the vertical stratification of leaves in a forest canopy is promoted by the coexistence of species with contrasting crown architectures and shade tolerance, implying complementarity in spatial distribution of foliage and thus maximizing light interception in mixtures (9, 49). Together with these previous findings, our study underlines the importance of studying horizontal, vertical, and 3D dimensions to comprehensively understand the role of multifaceted aspects by which CSC can mediate positive biodiversity–productivity relationships (8, 54).

Complementarity Underpins the Modification by CSC of the Effects of Tree Species Richness on Aboveground Biomass. Our results revealed significant positive relationships between the three CSC indices (i.e., canopy cover, FHD, and box dimension) and net biodiversity effects or CEs across the 4 y, but not with SEs. These results indicate that the positive biodiversity–productivity relationships identified in this decade-old, large subtropical forest experiment were predominantly driven by species complementarity. Species partitioning in the horizontal and vertical dimensions leads to a more complete occupation of canopy space and light capture (48, 55) in more species-rich mixtures (8, 36, 43), which contributes to aboveground overyielding. The linear increase of the positive relationships of canopy cover, FHD, and box dimension with CEs over the 4 y suggests that species complementarity and niche partitioning in developing forest communities takes time. This result can be reconciled with contrasting findings of Williams et al., (10), obtained from younger communities where physical crown complementarity was still more closely related to SEs rather than CEs: Over time, competitive hierarchies as indicated by SEs are replaced by niche partitioning between species.

So far, only a few studies reporting results from forest biodiversity experiments have statistically partitioned the contribution of CEs and SEs to net biodiversity effects (2, 7), although the contributions of species complementarity and niche partitioning to biodiversity effects have been commonly inferred from ecological theory (56). For instance, a recent study in a temperate tree biodiversity experiment indicated that SEs may largely explain biodiversity effects, but it focused on detecting the spectral signatures of overyielding rather than directly contrasting SEs and CEs (57). Furthermore, previous studies reported results obtained during the first years of forest biodiversity experiments; and often covering a narrower tree species richness gradient than ours (7, 10). In our experiment, SEs were also more prominent during the first years but then gave way to CEs (2). This was explained by the relatively slow process of canopy filling during which trees progressively expand their crowns, gradually filling canopy space (58, 59). Overall, our study suggests that the mediation by CSC of tree species richness effects on community aboveground biomass is driven by species complementarity, which promotes niche partitioning in diverse tree canopies, and becomes increasingly important over time.

Limitations. In this study, the highest tree richness level (24 species) increased forest biomass by 89% compared to monocultures in 2024. While substantial, this effect is relatively lower than that observed in long-term grassland experiments, e.g., a nearly 200% increase in 16-species mixtures compared to monocultures after 13 y at the Cedar Creek grassland experiment (55, 60). This discrepancy may reflect some differences between forest and grassland biodiversity experiments. Trees typically have longer life histories than herbaceous plants, and are planted with much wider spacing, which delays the interactions such as competition and facilitation and the emergence of positive diversity effects. The planted forest at BEF-China is still relatively young (≤ 15 y), and the positive diversity effects on productivity are continuously increasing over time, which may partially explain the relatively lower diversity effects than that in the mentioned grassland experiment. Furthermore, the strongly positive relative diversity

effects on productivity in grassland experiments at least in part can be explained by declining monoculture productivity over the long term (60–63). Since productivity in our experimental forest plots does not yet show such declines at the lowest richness levels, diversity effects are only due to increased mixture productivity without contributions of decreased monoculture productivity. It may take much more time before monocultures deteriorate and stronger tree diversity effects fully emerge.

Additionally, while the use of UAV-borne LiDAR allowed us to conduct accurate measurements over multiple years, to avoid circularity in our models, we did not use LiDAR data to derive tree or forest biomass but rather relied on regular field measurements of monitored trees in this experiment and allometric calculation of aboveground biomass. The need to conduct these in situ measurements limits the possible scale of this approach. Other studies have used multimodal remote sensing to assess biodiversity–productivity relationships (64), and this may be a way to scale up more mechanistic studies like ours further while avoiding circular reasoning. As stated in the introduction, CSC may not always show a positive relationship with forest biomass accumulation and overyielding. This relationship is likely to depend on the growth stage of the trees as well as on the successional or ecological stage of the forest, and possibly on the number and identity of species (65, 66). Further studies are needed to investigate the CSC effects at later successional stages, when the older forest are more affected by the impact of light exclusion on the understory (37). Moreover, a particular species composition, likely even one not included in the experiment, may have highest productivity under the particular environmental conditions at the site over the 4-y observation period. However, to find this composition would require all species compositions to be tested (67); and yet it would still be possible that under different environmental conditions different particular species compositions would have highest performance (68), leaving foresters with the general recommendation of planting high-diversity mixtures as best strategy. Finally, we infer the importance of CSC from its apparent power to explain the causal relationship between tree species richness, a variable that was here experimentally manipulated, and community aboveground biomass. Methods to directly manipulate CSC independently of tree species richness and, ideally, independently of other covariates such as the diversity of other functional traits, are difficult to achieve but could provide a rigorous test of our conclusions.

Conclusions and Outlook. Although several studies have investigated relationships between species diversity and productivity in forests (7, 33, 47), the role of CSC in modulating biodiversity–productivity relationships and their change over time have rarely been quantified. Our study experimentally demonstrates that CSC—including the horizontal distribution and vertical stratification as well as holistic 3D CSC—can largely explain positive biodiversity–productivity relationships in a subtropical forest biodiversity experiment during early stand development (age 11/12 to 14/15 after planting). Additionally, we find that the overyielding observed in mixtures can be explained by the positive relationships between CEs and CSC, with these positive effects consistently strengthening across 4 y. This finding further enriches the existing niche partitioning theory (13, 35, 69). Within 4 y, CSC exhibited a consistent and strengthening trend in promoting CEs, suggesting that as stand age increases, the role of CSC in regulating biodiversity–productivity relationships also increases. Furthermore, compared with traditional field-based approaches, our study integrates remote sensing (UAV-borne LiDAR) with field data to efficiently build a comprehensive picture of how the 3D structure of forests underpins biodiversity–productivity relationships across more than 400 plots of a large forest biodiversity experiment. This integration enhances our ability to understand forest and ecosystem dynamics and facilitates cross-scale and cross-system comparisons (3, 4).

In summary, our study provides insights into the relationships between biodiversity and ecosystem functioning in plant communities with complex aboveground structures and highlights the importance of CSC in explaining tree productivity. By using UAV-borne LiDAR to obtain precise horizontal, vertical, and 3D canopy structural parameters in a large biodiversity manipulation experiment, we demonstrate how tree species richness increases CSC and how CSC relates to increased community aboveground biomass and biodiversity CEs. This approach holds potential for scaling up to broader spatial extents by using multiplatform and multimodal remote sensing technique, enabling efficient monitoring of forest structure dynamics and their impacts on ecosystem functioning, particularly in the context of anthropogenic disturbance and climate change. Given the likely strong contribution of CSC to bending the curve of forest loss and sustaining forest ecosystem functions (6, 33), our study emphasizes the need to consider CSC and its mediator role in biodiversity effects to promote biomass production, carbon storage, and thus contribute to climate change mitigation in long-term afforestation projects.

Materials and Methods

Study Site and Experimental Design. This study was conducted at the Biodiversity–Ecosystem Functioning Experiment China Platform (BEF-China) in Xingangshan, Dexing, Jiangxi Province (29°05′00″ to 29°07′43″ N, 117°54′19″ to117°55′53″ E). BEF-China is located in a highly diverse subtropical forest in southeast China, characterized by a mean annual temperature of 16.7 °C and an average annual precipitation of 1821 mm. Forest plots, each covering an area of 1 mu (25.8 × 25.8 m^2, i.e., 0.067 ha), were established at two sites (site A in 2009 and site B in 2010) by planting 400 individuals in a square grid design of 20 × 20 trees. Using a pool of 40 tree species, tree species richness of plots ranges from monocultures to 2-, 4-, 8-, 16-, and 24-species mixtures, following a "broken-stick" design across the two sites (2, 41), ensuring that all species occur at all diversity levels with the same number of individuals. For this study, among the 492 designed plots we used 482 plots, excluding 10 plots with unsuccessful tree establishment. Specifically, this dataset consisted of 159 plots with monocultures and 131, 92, 52, 38, and 10 plots with 2, 4, 8, 16, and 24-species mixtures, respectively.

Aboveground Biomass. To minimize edge effects, ecosystem functions were measured in the center of plots, excluding trees along the margins (2, 41). As all plots in the BEF-China experiment were planted with equal community density, population sizes per species decrease inversely with increasing species richness under a substitutive design (41). To ensure both representative sampling and consistency across richness gradients, the center of the plot was defined as the central 6 × 6 planting positions in monocultures and 2-species mixtures or the central 12 × 12 planting positions in 4-, 8-, 16-, and 24-species mixtures. This design balances the need to sample a comparable number of individuals per species to improve the precision of community biomass estimates while avoiding edge-related artifacts when including all 20 × 20 planting positions (41). From 2021 to 2024, i.e., age 12 to 15 of site A and age 11 to 14 of site B, we measured the basal diameter (BD) and the height (H) of all surviving trees in the center of each plot. The aboveground biomass (kg) of surviving tree individuals was calculated using the same allometric equation $H \times \pi (BD)^2 \times WD \times CF$ for all tree species to avoid artifacts due to species identity effects in subsequent analysis. WD refers to a general wood density of 0.52 for all species. CF is a correction factor of 0.5 (to account for the noncylindrical shape of trees), which is an average value for the young subtropical trees in BEF-China experiment (2, 70). The accumulated aboveground biomass (Mg ha^{-1}) was calculated annually as the aggregated aboveground biomass of the surviving individual trees in each plot center.

Biodiversity Effects. The net biodiversity effect can be mathematically separated into additive parts that represent the CE and SE (13). Mathematically, using yield as example, the SE is calculated as the covariance between the monoculture yield of species and their change in relative yield from monoculture to mixture multiplied by the number of species in mixture. The CE is calculated as the mean change in relative yield from monoculture to mixture multiplied by the mean monoculture value multiplied by the number of species in mixture. Using the additive partitioning method of Loreau and Hector (13), we decomposed the net biodiversity effect of productivity measures into the CE and the SE for each year and each mixture plot separately based on the following equation:

$$\Delta Y = \sum_i \Delta R_{Y_i} \times M_i = N \times \overline{\Delta R_Y} \times \overline{M} + N \times cov\left(\Delta R_Y, M\right), \quad [1]$$

where ΔR_{Y_i} is the change in relative yield from monoculture to mixture (deviation from expected relative yield in mixture) for species i, M_i is the yield of species i in monoculture, and N is the number of species in the mixture. In this equation, $N \times \overline{\Delta R_Y} \times \overline{M}$ quantifies the CE, and $N \times cov\left(\Delta R_Y, M\right)$ quantifies the SE. The sum of the two, ΔY, is the net biodiversity effect, the difference between the mixture yield and the average monoculture yield of the species contained in the mixture.

UAV-Borne LiDAR Data. Here, we acquired drone-based LiDAR data during the leaf-on seasons of September 2021–2024 using a Hesai Pandar 40P laser scanner (LiAir 220 N system, GreenValley International). Hesai Pandar 40P is a LiDAR sensor characterized by its 40-channel design, with a maximum range of 200 m at 10% reflectivity. It offers a vertical field of view of 40° (−25° to +15°), and horizontal resolutions of 0.2° at 10 Hz and 0.4° at 20 Hz. The vertical resolution is 0.33°. The sensor exhibits a minimum vertical error of 0.33° and a horizontal error of 0.2°, and the typical beam divergence is around 0.177° (3 mrad). It uses a rotation of the LiDAR sensor for scanning, enabling the acquisition of dense 3D point cloud data. The drone flew at an average altitude of 100 m above the ground and at a velocity of 8 m s^{-1}, resulting in an average point density > 105.9 points m^{-2}. Most flight lines overlapped > 50% and the maximum scan angle was ±15°. The LiDAR data were preprocessed following a standardized workflow, which included outlier removal, noise filtering, classification, and normalization (6). Briefly, outlier removal aimed to mitigate the influence of noise caused by high-flying objects (e.g., birds and powerlines) and multipath effects, which were identified by determining whether the distance between a point and its neighboring points exceeded a threshold of 4 SD of point distances. Filtering was used to classify LiDAR points into ground and nonground points. The point clouds were normalized using a 0.5-m digital elevation model (DEM) derived from ground points to minimize the impact of terrain elevations on LiDAR points. The elevation-normalized LiDAR point clouds were then used to estimate CSC indices at the plot level. All preprocessing steps were done using LiDAR360 software (GreenValley International, Beijing, China).

CSC. Forest CSC can be quantified with various structural attributes such as canopy height, leaf area, and leaf density (71). In this study, we selected canopy cover, FHD, and box dimension (D_b) as the three main CSC indices–these being of ecological relevance and measurable using UAV-borne LiDAR–to represent different facets of forest properties, including, respectively, the horizontal arrangement, vertical variance, and holistic complexity of canopy elements within the canopy space.

Canopy cover, FHD, and box dimension were computed for each plot using elevation-normalized LiDAR point clouds collected from 2021 to 2024. Canopy cover was approximately the inverse of the gap fraction and estimated as the proportion of the ground covered by forest canopy in percentage (19, 72).

FHD functions as a metric of variation and the number of canopy layers, representing the canopy vertical complexity, which forms the second axis of the canopy structure model (73, 74). FHD was calculated as the per-voxel relative leaf area density values of vegetation in 1-m layers, based on Shannon's entropy index (75):

$$FHD = -\sum_i p_i \times \ln\ p_i, \quad [2]$$

where p_i is the proportion of the total foliage which lies in the i^{th} of the chosen horizontal canopy layers. Here, we used a 1-m vertical interval and excluded the lowest 3 m (NFI definition of minimal forest height) to separate the understory from the canopy. These two CSC indices were computed using the "slidaRtools" (22) and "leafR" (76) R packages.

For each plot, the holistic 3D CSC was directly measured based on the UAV-borne LiDAR point clouds using the box dimension approach (26, 27). In fractal analysis, the box-counting dimension, also known as the Minkowski–Bouligand dimension, is more generally used to summarize the structural heterogeneity and complexity of a forest stand (77). The point cloud was transferred into voxel grids of varying sizes, typically beginning with the smallest bounding cube (box) that encloses the entire point cloud as one large voxel representing the stand. Subsequently, the voxel size (r) is progressively reduced, allowing the structures to be resolved in increasing detail (28). The box dimension was calculated as the slope of the fitted line (least square fit) through a plot of ln(N) over ln(1/r):

$$D_b = \lim_{r \to 0} \frac{ln\ N}{ln\left(\frac{1}{r}\right)}, \quad [3]$$

where N is the number of boxes of size r needed to enclose all points of the experimental plots. Considering the area and maximum tree height of each plot, our study started with a 30 × 30 × 30 m box, followed by the size of 15 × 15 × 15 m, and so on, until the lower cut-off was reached. The lower cut-off was set to 50 cm, which represents a highly conservative estimate of the point cloud resolution.

Statistical Analysis. Before model fitting, tree species richness was log_2-transformed (logR) to linearize its relationships with response variables. This log–linear relationship is widely used to fit biodiversity–ecosystem functioning relationships as it often turns the nonlinear relationship of ecosystem functions with untransformed species richness into a linear one, an expectation also reflected in the log_2-series (1, 2, 4, 8, …) of manipulated species richness (2, 41, 78). Linearity of a productivity–log_2-richness relationship indicates that each doubling of species numbers increases productivity by a constant amount. Compared with fitting higher-order polynomials to richness, log-transformation simplifies model structure while preserving explanatory power (60, 79). Note that this transformation was not intended to normalize residuals, but to reflect theoretical expectations of diminishing returns with increasing richness and to ensure comparability with previous BEF experiments (2, 78).

To test hypothesis 1 (H1), we used linear mixed models (LMMs) to examine the relationships between tree species richness and CSC indices (i.e., canopy cover, FHD, and box dimension) across the 4 y. We sequentially fitted site, logR, year (Y, linear), and the interaction of species richness and year (logR × Y) as fixed-effects explanatory terms. Plot was included as a random-effects term in the model:

$$C = \alpha + \beta_1 \cdot S + \beta_2 \cdot log\ R + \beta_3 \cdot Y + \beta_4 \cdot log\ R \times Y + \gamma_{Plot} + \varepsilon, \quad [4]$$

where C is the CSC index; S is site; $logR$ is log_2-transformed tree species richness; Y is year; α is the intercept and $\beta_{1,2,3,4}$ are the coefficients to be estimated; γ_{Plot} is the random effect term of plot; ε is the residual error.

For hypothesis 2-1 (H2-1), we used LMMs to examine the relationships between CSC indices and community aboveground biomass across the 4 y. We sequentially fitted site, CSC indices, year (Y, linear), and the interaction of CSC and year (C × Y) as fixed-effects explanatory terms. Plot was included as a random-effects term in the model:

$$B = \alpha + \beta_1 \cdot S + \beta_2 \cdot C + \beta_3 \cdot Y + \beta_4 \cdot C \times Y + \gamma_{Plot} + \varepsilon, \quad [5]$$

where B is the plot-level tree biomass; S is site; C means the CSC index; Y is year; α is the intercept and $\beta_{1,2,3,4}$ are the coefficients to be estimated; γ_{Plot} is the random effect term of plot; ε is the residual error.

We used LMMs and structural equation modeling (SEM) to test hypothesis 2-2 (H2-2), i.e., whether tree species richness increased aboveground biomass via multifaceted canopy structures. Based on the original field-measured aboveground biomass, we calculated the "modified" aboveground biomass by extracting the residuals from the models after accounting for the effects of CSC indices. We sequentially fitted CSC indices, site, logR, year (Y, linear), the interaction of CSC and year (C × Y), and the interaction of logR and year (logR × Y) as fixed-effects explanatory terms. Plot and the plot-by-year interaction were included as random-effects terms in the model:

$$B = \alpha + \beta_1 \cdot C + \beta_2 \cdot S + \beta_3 \cdot log\ R + \gamma_{Plot} + \beta_4 \cdot Y + \beta_5 \cdot C \times Y + \beta_6 \cdot log\ R \times Y + \gamma_{Plot \times Y} + \varepsilon, \quad [6]$$

where B is the plot-level tree biomass; C means the CSC index ; S is site; $logR$ is $\log_2$-transformed tree species richness; Y is year; α is the intercept and $\beta_{1,2,3,4,5,6}$ are the coefficients to be estimated; γ_{Plot} and $\gamma_{Plot\times Y}$ are the random effect terms of plot and the interaction between plot and Y to test the significance of previous terms in the same way as in ordinary mixed models (80); ε is the residual error.

We used structural equation models (SEMs) to further examine the role of multifaceted CSC in mediating the effect of tree diversity on community productivity using the piecewiseSEM package (81). We fitted SEM to test the relationships between tree species richness, box dimension, and aboveground biomass. The SEM initially included all potential variables, with the paths indicated by hypothesis 2–2 and all other plausible paths (*SI Appendix*, Fig. S2*A*). Models were simplified by removing the nonsignificant or least-significant paths in a stepwise procedure (82) and the final model was selected based on Fisher's C statistic ($P > 0.05$ for a satisfactory fit) and Akaike information criterion (AIC) values (81).

We also fitted a SEM to test the relationships between tree species richness, horizontal (canopy cover) and vertical (FHD) CSC indices, and aboveground biomass. Similarly, the SEM initially included all potential variables (*SI Appendix*, Fig. S3*A*). In both 2023 and 2024, we ultimately adopted a saturated SEM that retained all hypothesized pathways (Fig. 4*B* and *SI Appendix*, Fig. S3*D*). As saturated models have no residual degrees of freedom, conventional global goodness-of-fit indices (e.g., Fisher's C or χ^2 tests) are not applicable. Instead, we evaluated the model fitness based on AIC. The saturated model showed a substantially lower AIC compared to the unsaturated model (ΔAIC = −13.96; 4610.2 vs. 4624.2), indicating better fitness. Additionally, a chi-square difference test confirmed the significantly improved fit of the saturated model (χ^2_diff = 15.96, df = 1, $P < 0.001$; *SI Appendix*, Tables S9 and S10). We therefore retained the saturated model as the final model for interpretation. We also assessed individual path significance and R^2 values, which together supported the robustness of the final model.

Finally, to test hypothesis 3 (H3), we used LMMs to examine the relationships between CSC indices and biodiversity effects (i.e., net biodiversity effects, CEs and SEs) across the 4 y. We sequentially fitted site, CSC indices, year (Y, linear), and the interaction of CSC and year (C × Y) as fixed-effects explanatory terms. Plot was included as a random-effects term in the model:

$$D = \alpha + \beta_1 \cdot S + \beta_2 \cdot C + \beta_3 \cdot Y + \beta_4 \cdot C \times Y + \gamma_{Plot} + \varepsilon, \quad [7]$$

where D is the plot-level biodiversity effect; S is site; C means the CSC index; Y is year; α is the intercept and $\beta_{1,2,3,4}$ are the coefficients to be estimated; γ_{Plot} is the random effect term of plot; ε is the residual error.

Then we analyzed the bivariate relationships between CSC indices and biodiversity effects for each year of the experiment. We extracted the coefficients of these relationships as indicators of effect size, the corresponding standard error as a measure of precision, and the P-value as indicator of significance.

We also used LMMs to examine the relationships between tree species richness and biodiversity effects (i.e., net biodiversity effects, CEs and SEs) across the 4 y. We sequentially fitted site, logR, year (Y, linear), and the interaction of species richness and year (logR × Y) as fixed-effects explanatory terms. Plot was included as a random-effects term in the model:

$$D = \alpha + \beta_1 \cdot S + \beta_2 \cdot log\ R + \beta_3 \cdot Y + \beta_4 \cdot log\ R \times Y + \gamma_{Plot} + \varepsilon, \quad [8]$$

where D is the plot-level biodiversity effect; S is site; $log\ R$ is $\log_2$-transformed tree species richness; Y is year; α is the intercept and $\beta_{1,2,3,4}$ are the coefficients to be estimated; γ_{Plot} is the random effect term of plot; ε is the residual error. All statistical analyses were conducted in R 4.2.1 (83).

Data, Materials, and Software Availability. The datasets and codes used for this study are available at Figshare (https://doi.org/10.6084/m9.figshare.29592203) (84).

ACKNOWLEDGMENTS. We acknowledge the management team of Biodiversity–Ecosystem Functioning Experiment China (BEF-China) platform for their great efforts in experiment maintenance and plot inventory. This study was supported by the National Key Research Development Program of China (2022YFF0802300), the National Natural Science Foundation of China (32222055, 32525042), and the Youth Innovation Promotion Association of the Chinese Academy of Sciences (2023019). T.R. was supported by the International Research Training Group TreeDì (GRK2324) jointly funded by the Deutsche Forschungsgemeinschaft (German Research Foundation)–319936945 and the University of Chinese Academy of Science.

Author affiliations: [a]State Key Laboratory of Forage Breeding-by-Design and Utilization, Key Laboratory of Vegetation and Environmental Change, Institute of Botany, Chinese Academy of Sciences, Beijing 100093, China; [b]University of Chinese Academy of Sciences, Beijing 100049, China; [c]Remote Sensing Laboratories, Department of Geography, University of Zurich, 8057 Zurich, Switzerland; [d]Institute of Biology/Geobotany and Botanical Garden, Martin Luther University Halle-Wittenberg, 06108 Halle, Germany; [e]German Centre for Integrative Biodiversity Research Halle-Jena-Leipzig, 04103 Leipzig, Germany; [f]Institute of General Ecology and Environmental Protection, Technische Universität Dresden, 01737 Tharandt, Germany; [g]Department of Chemistry, University of Zurich, 8057 Zurich, Switzerland; and [h]Zhejiang Qianjiangyuan Forest Biodiversity National Observation and Research Station, Beijing 100093, China

1. J. Liang *et al.*, Positive biodiversity-productivity relationship predominant in global forests. *Science.* **354**, aaf8957 (2016).
2. Y. Huang *et al.*, Impacts of species richness on productivity in a large-scale subtropical forest experiment. *Science.* **362**, 80–83 (2018).
3. E. A. LaRue *et al.*, A theoretical framework for the ecological role of three-dimensional structural diversity. *Front. Ecol. Environ.* **21**, 4–13 (2023).
4. T. Jucker, Deciphering the fingerprint of disturbance on the three-dimensional structure of the world's forests. *New Phytol.* **233**, 612–617 (2022).
5. J. W. Atkins, R. T. Fahey, B. S. Hardiman, C. M. Gough, Forest canopy structural complexity and light absorption relationships at the subcontinental scale. *J. Geophys. Res. Biogeosci.* **123**, 1387–1405 (2018).
6. X. Liu *et al.*, Enhancing ecosystem productivity and stability with increasing canopy structural complexity in global forests. *Sci. Adv.* **10**, eadl1947 (2024).
7. T. Ray *et al.*, Tree diversity increases productivity through enhancing structural complexity across mycorrhizal types. *Sci. Adv.* **9**, eadi2362 (2023).
8. M. Kunz *et al.*, Neighbour species richness and local structural variability modulate aboveground allocation patterns and crown morphology of individual trees. *Ecol. Lett.* **22**, 2130–2140 (2019).
9. J. Guillemot *et al.*, Neighbourhood-mediated shifts in tree biomass allocation drive overyielding in tropical species mixtures. *New Phytol.* **228**, 1256–1268 (2020).
10. L. J. Williams, A. Paquette, J. Cavender-Bares, C. Messier, P. B. Reich, Spatial complementarity in tree crowns explains overyielding in species mixtures. *Nat. Ecol. Evol.* **1**, 0063 (2017).
11. T. Ray *et al.*, Diversity-enhanced canopy space occupation and leaf functional diversity jointly promote overyielding in tropical tree communities. *Sci. Total Environ.* **951**, 175438 (2024).
12. T. Van de Peer, K. Verheyen, Q. Ponette, N. N. Setiawan, B. Muys, Overyielding in young tree plantations is driven by local complementarity and selection effects related to shade tolerance. *J. Ecol.* **106**, 1096–1105 (2018).
13. M. Loreau, A. Hector, Partitioning selection and complementarity in biodiversity experiments. *Nature.* **412**, 72–76 (2001).
14. J. Ruijven, F. Berendse, Diversity-productivity relationships: Initial effects, long-term patterns, and underlying mechanisms. *Proc. Natl. Acad. Sci.* **102**, 695–700 (2005).
15. B. J. Cardinale *et al.*, Impacts of plant diversity on biomass production increase through time because of species complementarity. *Proc. Natl. Acad. Sci.* **104**, 18123–18128 (2007).
16. J. Fargione *et al.*, From selection to complementarity: Shifts in the causes of biodiversity-productivity relationships in a long-term biodiversity experiment. *Proc. Biol. Sci.* **274**, 871–876 (2007).
17. F. J. Bongers *et al.*, Functional diversity effects on productivity increase with age in a forest biodiversity experiment. *Nat. Ecol. Evol.* **5**, 1594–1603 (2021).
18. G. Hui, G. Zhang, Z. Zhao, A. Yang, Methods of forest structure research: A review. *Curr. Forestry Rep.* **5**, 142–154 (2019).
19. J. W. Atkins *et al.*, Scale dependency of lidar-derived forest structural diversity. *Methods Ecol. Evol.* **14**, 708–723 (2023).
20. B. S. Hardiman, G. Bohrer, C. M. Gough, C. S. Vogel, P. S. Curtis, The role of canopy structural complexity in wood net primary production of a maturing northern deciduous forest. *Ecology.* **92**, 1818–1827 (2011).
21. N. C. Coops *et al.*, Modelling lidar-derived estimates of forest attributes over space and time: A review of approaches and future trends. *Remote Sens. Environ.* **260**, 112477 (2021).
22. N. Knapp, R. Fischer, V. Cazcarra-Bes, A. Huth, Structure metrics to generalize biomass estimation from lidar across forest types from different continents. *Remote Sens. Environ.* **237**, 111597 (2020).
23. Q. Guo *et al.*, Lidar boosts 3d ecological observations and modelings: A review and perspective. *IEEE Geosci. Remote Sens. Mag.* **9**, 232–257 (2021).
24. F. Morsdorf, D. Kükenbrink, F. D. Schneider, M. Abegg, M. E. Schaepman, Close-range laser scanning in forests: Towards physically based semantics across scales. *Interface Focus.* **8**, 20170046 (2018).
25. B. Brede *et al.*, Non-destructive tree volume estimation through quantitative structure modelling: Comparing UAV laser scanning with terrestrial LIDAR. *Remote Sens. Environ.* **233**, 111355 (2019).
26. D. Seidel *et al.*, Deriving stand structural complexity from airborne laser scanning data–What does it tell us about a forest?. *Remote Sens.* **12**, 1854 (2020).
27. D. Seidel, A holistic approach to determine tree structural complexity based on laser scanning data and fractal analysis. *Ecol. Evol.* **8**, 128–134 (2018).
28. D. Da Silva *et al.*, "A critical appraisal of the box counting method to assess the fractal dimension of tree crowns, lecture notes" in *Computer Science, in Advances in Visual Computing*, G. Bebis *et al.*, Eds. (Springer, Berlin Heidelberg, 2006), pp. 751–760.
29. S. Getzin, K. Wiegand, I. Schöning, Assessing biodiversity in forests using very high-resolution images and unmanned aerial vehicles. *Methods Ecol. Evol.* **3**, 397–404 (2012).
30. W. Turner, Sensing biodiversity. *Science.* **346**, 301–302 (2014).
31. D. C. Zemp *et al.*, Mixed-species tree plantings enhance structural complexity in oil palm plantations. *Agric. Ecosyst. Environ.* **283**, 106564 (2019).
32. C. Fahey *et al.*, Canopy complexity drives positive effects of tree diversity on productivity in two tree diversity experiments. *Ecology* **106**, e4500 (2025).

33. T. C. Coverdale, A. B. Davies, Unravelling the relationship between plant diversity and vegetation structural complexity: A review and theoretical framework. *J. Ecol.* **111**, 1378–1395 (2023).
34. H. Pretzsch, Canopy space filling and tree crown morphology in mixed-species stands compared with monocultures. *For Ecol Manage.* **327**, 251–264 (2014).
35. P. A. Niklaus, M. Baruffol, J.-S. He, K. Ma, B. Schmid, Can niche plasticity promote biodiversity–productivity relationships through increased complementarity?. *Ecology.* **98**, 1104–1116 (2017).
36. M. D. Perles-Garcia, M. Kunz, A. Fichtner, W. Härdtle, G. Von Oheimb, Tree species richness promotes an early increase of stand structural complexity in young subtropical plantations. *J. Appl. Ecol.* **58**, 2305–2314 (2021).
37. X. Yi *et al.*, From canopy complementarity to asymmetric competition: The negative relationship between structural diversity and productivity during succession. *J. Ecol.* **110**, 457–465 (2022).
38. L. Zhai, R. E. Will, B. Zhang, Structural diversity is better associated with forest productivity than species or functional diversity. *Ecology* **105**, e4269 (2024).
39. D. Binkley, O. C. Campoe, M. Gspaltl, D. I. Forrester, Light absorption and use efficiency in forests: Why patterns differ for trees and stands. *For. Ecol. Manage.* **288**, 5–13 (2013).
40. B. Schmid, The species richness–productivity controversy. *Trends Ecol. Evol.* **17**, 113–114 (2002).
41. H. Bruelheide *et al.*, Designing forest biodiversity experiments: General considerations illustrated by a new large experiment in subtropical China. *Methods Ecol. Evol.* **5**, 74–89 (2014).
42. A. T. Fotis *et al.*, Forest structure in space and time: Biotic and abiotic determinants of canopy complexity and their effects on net primary productivity. *Agric. For. Meteorol.* **250–251**, 181–191 (2018).
43. T. Jucker, O. Bouriaud, D. A. Coomes, Crown plasticity enables trees to optimize canopy packing in mixed-species forests. *Funct. Ecol.* **29**, 1078–1086 (2015).
44. X. Morin, Species richness promotes canopy packing: A promising step towards a better understanding of the mechanisms driving the diversity effects on forest functioning. *Funct. Ecol.* **29**, 993–994 (2015).
45. Q. Ma *et al.*, The coordinated impact of forest internal structural complexity and tree species diversity on forest productivity across forest biomes. *Fundam. Res.* **4**, 1185–1195 (2024).
46. K. Siegel, L. E. Dee, Foundations and future directions for causal inference in ecological research. *Ecol. Lett.* **28**, e70053 (2025).
47. C. M. Gough, J. W. Atkins, R. T. Fahey, B. S. Hardiman, High rates of primary production in structurally complex forests. *Ecology* **100**, e02864 (2019).
48. L. J. Williams *et al.*, Enhanced light interception and light use efficiency explain overyielding in young tree communities. *Ecol. Lett.* **24**, 996–1006 (2021).
49. J. Sapijanskas, A. Paquette, C. Potvin, N. Kunert, M. Loreau, Tropical tree diversity enhances light capture through crown plasticity and spatial and temporal niche differences. *Ecology.* **95**, 2479–2492 (2014).
50. Z. Ma, H. Y. H. Chen, P. Kumar, B. Gao, Species mixture increases production partitioning to belowground in a natural boreal forest. *For. Ecol. Manage.* **432**, 667–674 (2019).
51. I. Laforest-Lapointe, A. Paquette, C. Messier, S. W. Kembel, Leaf bacterial diversity mediates plant diversity and ecosystem function relationships. *Nature.* **546**, 145–147 (2017).
52. Y. Li *et al.*, Multitrophic arthropod diversity mediates tree diversity effects on primary productivity. *Nat. Ecol. Evol.* **7**, 832–840 (2023).
53. X. Jing *et al.*, Climatic conditions, not above- and belowground resource availability and uptake capacity, mediate tree diversity effects on productivity and stability. *Sci. Total Environ.* **812**, 152560 (2022).
54. S. Martin-Blangy, C. Meredieu, H. Jactel, D. Bonal, M. Charru, Species-mixing effects on crown dimensions and canopy packing in a young pine–birch plantation are modulated by stand density and irrigation. *Eur. J. For. Res.* **142**, 197–216 (2023).
55. K. E. Mueller, D. Tilman, D. A. Fornara, S. E. Hobbie, Root depth distribution and the diversity–productivity relationship in a long-term grassland experiment. *Ecology.* **94**, 787–793 (2013).
56. Y. Wu *et al.*, Functional diversity explains ecosystem carbon storage in subtropical forests. *Glob. Change Biol.* **31**, e70120 (2025).
57. L. J. Williams *et al.*, Remote spectral detection of biodiversity effects on forest biomass. *Nat. Ecol. Evol.* **5**, 46–54 (2020).
58. J. Urgoiti *et al.*, No complementarity no gain–Net diversity effects on tree productivity occur once complementarity emerges during early stand development. *Ecol. Lett.* **25**, 851–862 (2022).
59. E. B. Searle, H. Y. H. Chen, Complementarity effects are strengthened by competition intensity and global environmental change in the central boreal forests of Canada. *Ecol. Lett.* **23**, 79–87 (2020).
60. D. Tilman, F. Isbell, J. M. Cowles, Biodiversity and ecosystem functioning. *Annu. Rev. Ecol. Evol. Syst.* **45**, 471–493 (2014).
61. P. B. Reich *et al.*, Impacts of biodiversity loss escalate through time as redundancy fades. *Science.* **336**, 589–592 (2012).
62. C. Wagg *et al.*, Biodiversity–stability relationships strengthen over time in a long-term grassland experiment. *Nat. Commun.* **13**, 7752 (2022).
63. S. T. Meyer *et al.*, Effects of biodiversity strengthen over time as ecosystem functioning declines at low and increases at high biodiversity. *Ecosphere* **7**, e01619 (2016).
64. Z. Zheng *et al.*, Remotely sensed functional diversity and its association with productivity in a subtropical forest. *Remote Sens. Environ.* **290**, 113530 (2023).
65. A. Ali, Forest stand structure and functioning: Current knowledge and future challenges. *Ecol. Indic.* **98**, 665–677 (2019).
66. T. Matsuo, M. Martínez-Ramos, F. Bongers, M. T. van der Sande, L. Poorter, Forest structure drives changes in light heterogeneity during tropical secondary forest succession. *J. Ecol.* **109**, 2871–2884 (2021).
67. B. Schmid, A. Hector, P. Saha, M. Loreau, Biodiversity effects and transgressive overyielding. *J. Plant Ecol.* **1**, 95–102 (2008).
68. F. Isbell *et al.*, High plant diversity is needed to maintain ecosystem services. *Nature.* **477**, 199–202 (2011).
69. O. Godoy, L. Gómez-Aparicio, L. Matías, I. M. Pérez-Ramos, E. Allan, An excess of niche differences maximizes ecosystem functioning. *Nat. Commun.* **11**, 4180 (2020).
70. F. Schnabel *et al.*, Species richness stabilizes productivity via asynchrony and drought-tolerance diversity in a large-scale tree biodiversity experiment. *Sci. Adv.* **7**, eabk1643 (2021).
71. M. Ehbrecht, P. Schall, C. Ammer, D. Seidel, Quantifying stand structural complexity and its relationship with forest management, tree species diversity and microclimate. *Agric. For. Meteorol.* **242**, 1–9 (2017).
72. N. Knapp, R. Fischer, A. Huth, Linking lidar and forest modeling to assess biomass estimation across scales and disturbance states. *Remote Sens. Environ.* **205**, 199–209 (2018).
73. R. T. Fahey *et al.*, Defining a spectrum of integrative trait-based vegetation canopy structural types. *Ecol. Lett.* **22**, 2049–2059 (2019).
74. F. D. Schneider *et al.*, Mapping functional diversity from remotely sensed morphological and physiological forest traits. *Nat. Commun.* **8**, 1441 (2017).
75. C. Shannon, A mathematical theory of communication. *Bell Syst. Tech. J.* **27**, 379–423 (1948).
76. D. R. A. D. Almeida, S. C. Stark, C. A. Silva, C. Hamamura, leafR: Calculates the Leaf Area Index (LAD) and Other Related Functions. https://doi.org/10.32614/CRAN.package.leafR. Deposited 11 June 2019.
77. B. B. Mandelbrot, The fractal geometry of nature. *Am. J. Phys.* **51**, 286–286 (1983).
78. A. Hector *et al.*, Plant diversity and productivity experiments in European grasslands. *Science.* **286**, 1123–1127 (1999).
79. B. Schmid *et al.*, "Consequences of species loss for ecosystem functioning: meta-analyses of data from biodiversity experiments" in *Biodiversity, Ecosystem Functioning, and Human Wellbeing*, Naeem, D. E. Bunker, A. Hector, M. Loreau, C. Perrings, Eds. (Oxford University PressOxford, 2009), pp. 14–29.
80. B. Schmid, M. Baruffol, Z. Wang, P. A. Niklaus, A guide to analyzing biodiversity experiments. *J. Plant Ecol.* **10**, 91–110 (2017).
81. J. S. Lefcheck, PiecewiseSEM: Piecewise structural equation modelling in R for ecology, evolution, and systematics. *Methods Ecol. Evol.* **7**, 573–579 (2016).
82. W. Xiao, C. Chen, H. Y. H. Chen, Nitrogen deposition suppresses soil respiration by reducing global belowground activity. *Sci. Total Environ.* **921**, 171246 (2024).
83. R Core Team, *R: A Language and Environment for Statistical Computing* (R Foundation for Statistical Computing, Vienna, Austria, 2022).
84. X. Liu, X. Deng, Data and code from "Forest biodiversity increases productivity via complementarity from greater canopy structural complexity." Figshare. https://doi.org/10.6084/m9.figshare.29592203. Deposited 18 July 2025.